Cold Flow Simulation in Underground Coal Gasification (UCG) Cavities

Dipankar Chatterjee[1,*], Satish Kumar Gupta[2], Chebolu Aravind[3] and Rakesh Roshan[3]

[1]*Simulation & Modeling Laboratory, CSIR-Central Mechanical Engineering Research Institute, Durgapur-713209, India*

[2]*Department of Mechanical Engineering, National Institute of Technology, Durgapur-713209, India*

[3]*Department of Mechanical Engineering, Indian Institute of Technology, Kharagpur-721302, India*

Abstract: Underground coal gasification (UCG), in the recent years, have gathered a significant amount of interest from the researchers because of its advantages over conventional mining and utilization techniques. It is one of the most promising and innovative technology where coal is gasified in-situ by injection of a suitable oxidant for the production of synthetic gas. The simultaneous occurrence of several phenomena such as complex flow patterns, chemical reactions, water influx, thermo-mechanical failure of the coal seam etc. make the mathematical modeling of the entire UCG process very abstruse and computationally challenging. The reaction between the oxidant and the coal in the deep underground seams leads to the formation of combustible gas and subsequently results in a cavity. As the gasification proceeds the cavity grows three dimensionally in a non-linear fashion. The cavity size strongly depends on several parameters like position and orientation of the inlet nozzle, coal properties etc. A comprehensive three-dimensional numerical study is conducted to understand the hydrodynamics within a given cavity size which would give us a relatively quick but reliable insights into the process. Five different cavity sizes are considered inside which the complete turbulent transport is simulated. Apart from the usual vertical and horizontal injection, the effect of inclined injection on the hydrodynamics is also reported here for the first time.

Keywords: Underground coal gasification, mathematical modeling, cavity growth, syngas.

1. INTRODUCTION

Coal is the most abundant and widespread type of fossil fuel and the total amount of coal reserves is reported to be 18 Teratonnes. However, only 850 Gigatonnes of it is estimated to be economically recoverable using current technologies. These coal reserves are discovered through exploration activities and mining is conventionally used to extract the recoverable coal from underground. Recent energy demands and stringent environmental regulations have forced us to look into other innovative, non-conventional and more efficient methods of coal extraction. Underground coal gasification (UCG) is one such methods in which unrecoverable coal is converted to syngas in-situ. The coal seams are gasified underground with the mixture of air/oxygen and steam and synthetic gas is produced for use in power generation or as chemical feed stock. It is similar to the surface gasification where syngas is produced through the same chemical reactions, however, the major difference lies in the fact that surface gasification occurs in a manufactured reactor whereas UCG occurs in a natural geological formation containing un-mined coal. Apart from being a less expensive method compared to conventional mining techniques, it also reduces the safety, health and environmental problems associated with deep mining. A thorough review on the environmental concerns of underground coal gasification is given by Imran *et al*. [1].

The UCG process involves vertically drilling of two holes, namely, injection and production wells from the surface to the coal seam up to a certain distance, connected by a permeable channel link. A mixture of air/oxygen and steam is introduced into the coal seam through the injection well. The syngas formed travels through the cavity and is collected at the surface from the production well. The cavity formed due to the formation of syngas grows three-dimensionally in a non-linear fashion. Several phenomena such as complex flow patterns, chemical reactions, water influx, thermo-mechanical failure of the coal seam, heat and mass transport, spalling and other geological phenomenon occur simultaneously which makes the entire UCG process very complex. It is worth mentioning that formation of cavity and its shape plays a major role in determining the success of the entire process both economically and environmentally. Its lateral dimensions influence resource recovery by determining the spacing between modules, and overall dimension guides the hydrological and subsidence response of the overburden.

*Address correspondence to this author at the Simulation & Modeling Laboratory, CSIR-Central Mechanical Engineering Research Institute, Durgapur-713209, India; Tel: +91-343-6510455; Fax: +91-343-2548204; E-mail: d_chatterjee@cmeri.res.in

E-ISSN: 2409-5826/14

Apart from being expensive and very difficult to envisage, field-scale experiments are invaluable at providing insights in to the phenomenon. On the other hand, laboratory experiments are feasible but their scalability is questionable. Hence, several researchers have developed mathematical models of the UCG process in order to mimic and understand the intricacies involved in it and a comprehensive review of the status quo is provided by Aghalayam [2]. Hadi and Hafez [3] deployed the finite element method to predict the changes of temperature, gas composition, pressure and coal consumption in the UCG process. Wachowicz *et al.* [4] performed an energy balance of thermal phenomena accompanying the coal gasification process in order to predict any changes to the chemical composition of the syngas. The modeling results were compared with the results from the experimental studies. Perkins and Sahajwalla [5] developed a two-dimensional axisymmetric CFD model that could simulate the combined effects of heat and mass transport and chemical reaction during the gasification process. Despite the simplifications, their model was able to provide significant insights into the transport and chemical reaction phenomena. Yang [6] studied the nonlinear seepage movement characteristics of fluid in underground coal gasification. He developed mathematical models of three-dimensional unstable and nonlinear seepage on the basis of a model experiment. His calculated results from the mathematical models were concordant with the experimentally measured ones. Yang [7] established mathematical models on the underground coal gasification in steep coal seams according to their storage conditions and features of gas production process. His study revealed that increasing of the length of the gasification channel improved the heating value of the gas. In another article, Yang [8] established the dynamic nonlinear coupling mathematical models on underground coal gasification of inclined seams and solved it deploying a finite volume method. He studied the mathematical functional relationship between the chemical reaction rate and every influencing factor and his simulation results conformed very well with the experimental values. Yang and Liu [9] developed mathematical models on heat and mass transfer in UCG according to the conservation law of momentum, mass, and energy and the features of the gas production process. They also introduced the methods to determine the main model parameters and solve the numerical model by means of the volume-control method. Prabu and Jayanti [10] experimentally studied the cavity formation in UCG for three configurations: (i) sublimation experiments in camphor simulating primarily the heat transfer aspects, (ii) bore hole combustion in Acacia nilotica wood bringing in chemical reaction into play, and (iii) bore hole combustion a coal block bringing into consideration the effect of ash on the cavity formation. Their results revealed that the cavity formation rates as well as the shape of the cavity are significantly affected by the oxidant flow rate. Daggupati *et al*. [11] studied the feasibility of in situ gasification of coal in a laboratory scale reactor set-up, under conditions relevant for field practice of UCG, using an oxygen–steam mixture as the feed gas. They also reported the effect of various design and operating parameters on the evolution of the gasification cavity along with the empirical correlations for the change in cavity volume and its dimensions in various directions. Prabhu and Jayanti [12] further performed a proximate analysis of the coal samples from various locations of the heat-affected zone (HAZ) during borehole combustion and gasification studies. Their article reports that there is a considerable change in the volatiles to fixed carbon ratio in the depth direction and that the extent of variation depends on the coal as well as on the conditions prevailing during the experiment. Parka and Edgar [13] developed an one-dimensional unsteady-state model to predict the movement of the cavity wall and drying front during the initial period of coal block gasification. Some other research articles [14-17] also discuss the intricacies involved in modeling the UCG process and cavity formation. Daggupati *et al*. [18] in another effort performed residence time distribution (RTD) studies in order to understand the velocity distribution and non-ideal flow patterns in UCG cavities. They developed a compartment model based on their RTD studies which was capable of offering a computationally less expensive and easier option for determining the UCG process performance at a given time (when used in a reactor-scale model using reactions). In a very recent article, Yang *et al*. [19] developed a thermal–mechanical coupled model using the ABAQUS software package to predict the heat transfer, the stress distributions and the consequent surface subsidence.

Although development of a complete process model for the entire UCG process involving the thermal transport and associated chemical reactions has been a major goal as it would qualify us in visualizing the phenomena occurring underground and predicting the product gas quality, simplified models are important nonetheless. Number of assumptions and simplifications make the model tractable. In the present study we aim to study the complexities in the

hydrodynamics involved in the process by a simplified three-dimensional modeling approach. Our focus lies in the flow visualization inside the cavity as the success of the entire process depends on the cavity size and formation. A critical examination of the influence of nozzle orientations on the flow patterns is also carried out. We perform three-dimensional numerical simulations on cavities of pre-defined shapes and sizes to determine the steady state flow patterns. It is worth mentioning that in this study we do not aim at developing a complete process model for UCG, however, as mentioned earlier this simplified hydrodynamic analysis enables us in providing valuable insights into the flow physics associated with the UCG process.

2. PHYSICAL PROBLEM AND MATHEMATICAL FORMULATION

Five different cavity sizes are chosen for each nozzle orientation (horizontal, vertical and inclined) based on the data available in the literature [11, 13 and 18]. Different views of the geometries of the cavity are shown in the Figure **1**. Size 0, size 1, size 2, size 3 and size 4 represent the cavities at times 0, 1, 3, 7 and 14 days, respectively from the beginning of the UCG trials. All the geometries are created and discretized by unstructured tetrahedral grid using the commercially available meshing software GAMBIT [20]. To capture the effect of stiff velocity gradients finer meshing is used near the inlet and outlet and walls. Dimensions of different cavities used in the study along with the total number of grid faces, nodes and cells are given in Table **1**. The grid parameters given in Table **1** are for the horizontal inclination of the inlet. The dimensions for all the nozzle orientations remain same, however, a difference of less than 3% exist between the grid sizes. This small difference does not affect the solution and thus can be neglected while comparing. It is to be mentioned that the grid spacing is selected after a comprehensive grid sensitivity analysis. The sensitivity analysis is carried out for cavity size 1 by varying the spacing from 0.06 to 0.02. Figure **2** is plotted to show the variation of the volume average velocity magnitude for different internal grid spacing for cavity size 1. It is observed that an internal spacing of 0.03 within the entire cavity is sufficiently small for obtaining an accurate flow field for cavity size 1. Any further refinement below the cell size of 0.03 does not affect the solution since there is no significant change in the velocity magnitude for smaller cell sizes as evident from Figure **2**.

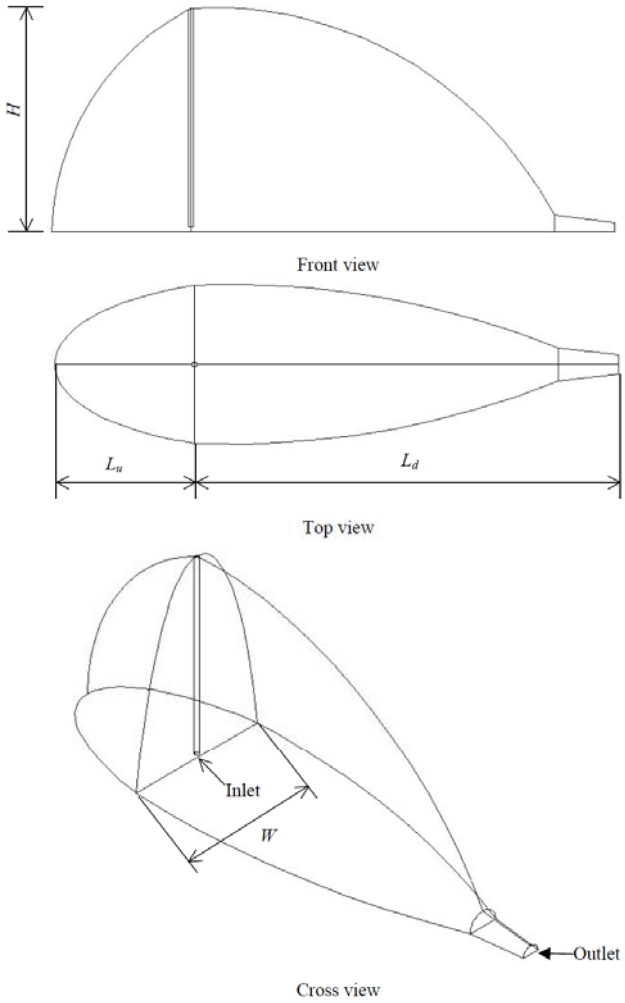

Figure 1: Geometry of UCG cavity for cavity size 4 (14 Days) for vertical injection.

2.1. Governing Equations

The governing equations for the three-dimensional incompressible flow with constant thermo-physical properties used to obtain the flow field can be expressed in the following forms:

Continuity Equation:

$$\nabla.\left(\rho\vec{v}\right)=0 \tag{1}$$

Momentum Equation:

$$\nabla.\left(\rho\vec{v}\vec{v}\right)=-\nabla p+\nabla.\left(\bar{\bar{\tau}}\right)+\rho\vec{g} \tag{2}$$

where $\vec{v}$ represents the velocity vector, p is the pressure, $\bar{\bar{\tau}}=\left(1/2\right)\mu\left[\Delta v+\left(\Delta v\right)^{T}\right]$ is the viscous stress tensor and $\vec{g}$ is the gravity vector along with the density ρ and dynamic viscosity μ.

Table 1: Dimensions of UCG Cavity for Different Sizes and their Grid Dimensions

Parameters	Size 0	Size 1	Size 2	Size 3	Size 4
Distance between production and injection well (m)	9.1	9.1	9.1	9.1	9.1
Length of cavity behind the inlet, L_u (m)	0.01	1	2	2.5	3
Length of the cavity dome from the inlet, L_d (m)	0	2.5	4	6	7.8
Height of the cavity, H (m)	0.2	1.32	2.2	3.2	4.7
Width of the cavity (m) at the injection well, W	0.2	0.9	1.5	2.2	3.3
Width of the cavity (m) at the outflow channel	0.2	0.3	0.42	0.52	0.7
Width of the cavity (m) at the backside of the injection well	0.2	0.25	0.3	0.4	0.6
Width of the cavity (m) at the outlet	0.2	0.2	0.25	0.3	0.4
Inlet and outlet diameter (m)	0.1	0.1	0.1	0.1	0.1
No. of grid faces	833721	2027564	3848806	5543751	8134934
No. of grid nodes	81300	182423	338449	481303	703039
No. of grid cells (tetrahedral and hexagonal)	403361	997973	1903378	2748727	4037189

The realizable $k-\varepsilon$ model [20] with standard wall function is used to model the turbulent transport.

The working fluid considered in the study is oxygen and its thermo-physical properties (refer to Table **2**) at a temperature of 1273 K is used for the simulation.

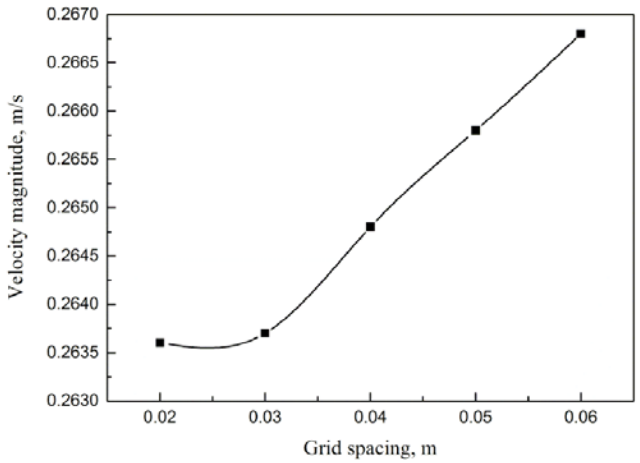

Figure 2: Grid independence test.

2.2. Boundary Conditions

At the inlet a uniform flow normal to the boundary is prescribed with a magnitude of 4 m/s. This mimics the condition of oxygen entering at a mass flow rate of 35.07 kg/h. A pressure boundary condition of 5 atm is implemented at the outlet. All the walls are considered at a temperature of 1273 K and a no-slip boundary condition prevails.

3. SOLUTION METHODOLOGY

The governing equations with aforementioned boundary conditions are solved by using the commercial CFD package FLUENT 6.0 [20]. FLUENT uses a control volume based technique to solve the governing system of partial differential equations in a collocated grid system by constructing a set of discrete algebraic equations. The pressure based numerical scheme, which solves the discretized governing equations sequentially, is selected. The sequence updates the velocity field through the solution of the momentum equations using known values for pressure and velocity. Then, it solves a 'Poisson-type' pressure correction equation obtained by combining the continuity and momentum equations. A second order upwind scheme is used for spatial discretization of the momentum equation. SIMPLE algorithm is selected as the pressure-velocity coupling scheme. The standard pressure interpolation technique is used to interpolate the face pressure from the cell center values. Finally, the algebraic equations are solved by using the Gauss-

Table 2: Properties of Oxygen at 1 Atm Pressure and 1273 K [21]

ρ **Density (kg/m^3)**	μ **Viscosity (10^{-7} Pa.s)**	k **Thermal conductivity (10^{-3} W/m-K)**	c_p **Specific heat (kJ/kg-K)**
0.302642	573.307	86.134	1.1223

Siedel point-by-point iterative method in conjunction with the Algebraic Multigrid (AMG) solver. The convergence criteria based on the relative error are set as 10^{-7} for the discretized continuity and momentum equations to ensure a well defined steady solution.

4. RESULTS AND DISCUSSION

In order to validate the present numerical method, first the simulation is done for cavity size 0 to obtain the residence time distribution (RTD) and compared with the reported result in the literature [18]. The RTD simulation is carried out after a steady state velocity profile is obtained inside the cavity. The velocity profile is then frozen and a virtual tracer element (which is considered to have properties similar to those of oxygen) is injected into the cavity to track the tracer movement. An unsteady species balance equation of the following form is solved to obtain the concentration of the tracer in the form of the area-weighted average at the outlet, and the result is plotted against time. This plot represents the residence time distribution (RTD) as shown in Figure **3**. The figure also shows the results from [18] and an excellent matching can be observed with the present computation.

$$\frac{\partial}{\partial t}\left(\rho Y_i\right) + \nabla.\left(\rho \vec{v} Y_i\right) = -\nabla.\vec{j}_i \tag{3}$$

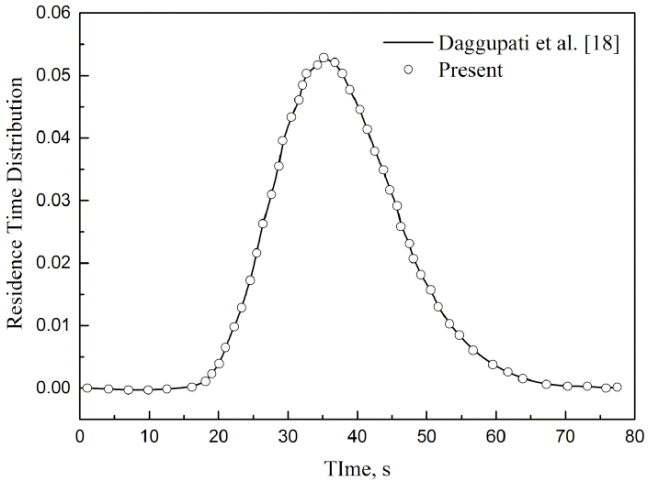

Figure 3: Residence time distribution for cavity size 0.

The effects of diffusion are minimized by considering the diffusivity of the tracer as 1×10^{-15} m^2/s. The tracer is injected as a pulse at the inlet with a mass fraction of 1.0.

In the present study, extensive three dimensional numerical simulations are carried out to understand the fluid dynamic transport within predefined UCG cavities. Particular emphasis is given to elucidate the role of different nozzle orientations on the flow pattern. The results are analyzed with the help of velocity contours, vectors and pathlines for clear understanding of the flow field. Figures **4-9** show the contours of velocity magnitude for different nozzle orientations at centre (x = 0) and vertical planes (z = 0) for different cavity sizes. The plots suggests that as the cavity size increases the overall average value of the velocity magnitude decreases irrespective of the type of injection. It is observed that in the case of vertical injection the flow distribution occurs around the inlet whereas for horizontal injection a significant parallel side-stream bypass occurs towards the outlet. A well mixed flow distribution is seen in the case of inclined injection. A closer look at the plots reveal that for the case of vertical injection the maximum velocity zones occur only near the inlet whereas for horizontal injection another maximum velocity zone is observed near the roof for all the cavity sizes. This can be attributed to the recycling of the stream from the entrance of the outflow channel. It is interesting to note that apart from the maximum velocity zone occurring near the top, other maximum velocity zones occur in the case of inclined injection. This occurs because inclined orientation of the nozzle imparts velocity in both x- and y-directions, resulting in maximum velocity zones also on the left side of the cavity.

Figure **10** shows the velocity vectors of inclined injection for a representative cavity of size 1 at different vertical planes to understand the phenomenon of back mixing. It is seen that back mixing is more prevalent in the zones near the injection nozzle, however, as one moves away from the nozzle (closer to the outflow channel) back mixing reduces. Figure **11** shows the pathlines for a representative cavity of size 1 for all the three nozzle orientations at different time steps. They basically demonstrate the path of an injected pulse from the inlet. For the case of horizontal injection a relatively larger portion of the pathlines behave like a parallel side stream and separately leave the cavity through the outflow channel independent of the cavity size. For the case of vertical injection the pathlines first hit the base of the cavity and the reflected pathlines leave the cavity through the outflow channel. They do not leave in the form of a stream as in the case of horizontal injection and a relatively better mixing is observed. The pathlines in the case of inclined injection show a combination of both the phenomena because of their velocity in both and x- and y-directions. They are well distributed and mixed.

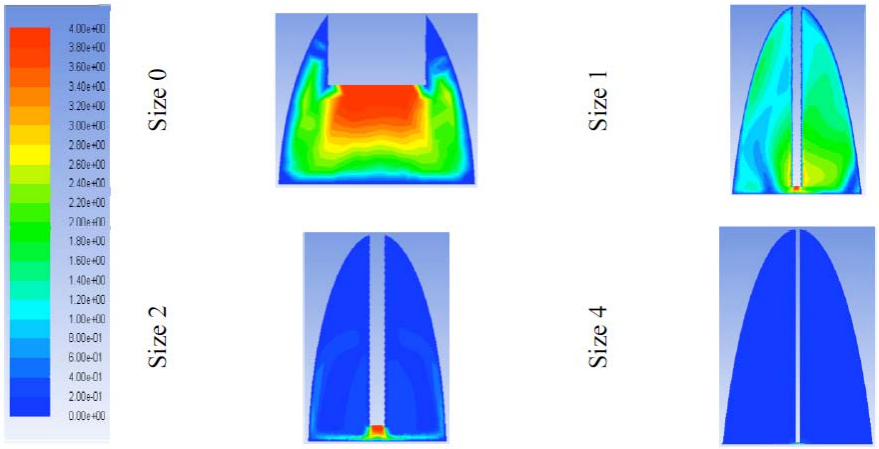

Figure 4: Velocity magnitude contours (in m/s) for vertical injection on a vertical plane at $x = 0$ for different cavity sizes.

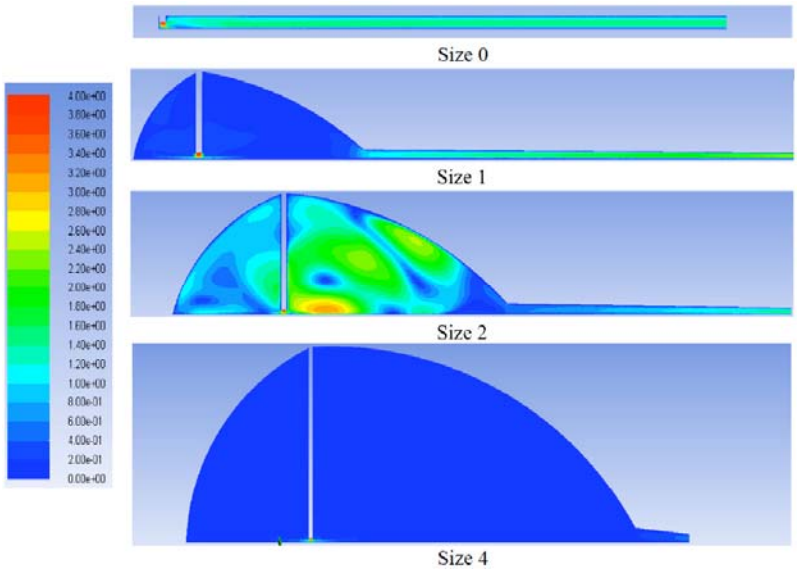

Figure 5: Velocity magnitude contours (in m/s) for vertical injection on a center plane at $z = 0$ for different cavity sizes.

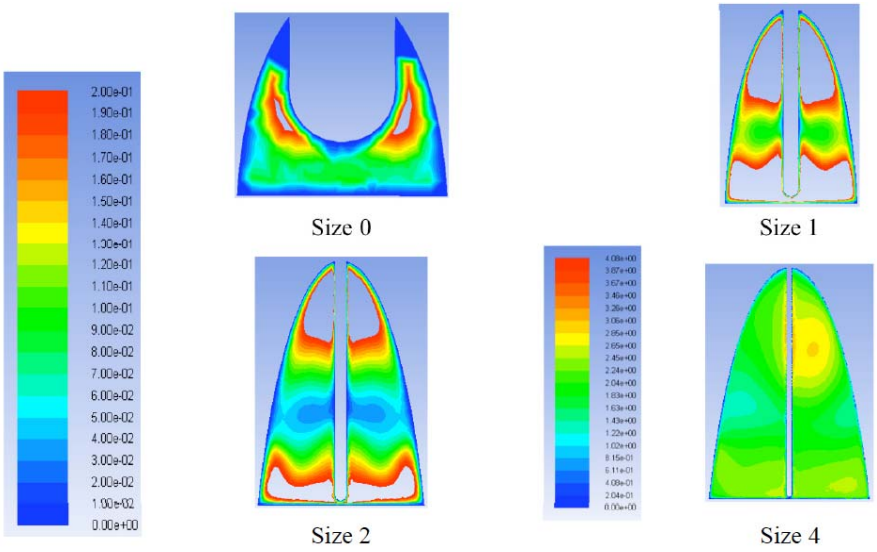

Figure 6: Velocity magnitude contours (in m/s) for horizontal injection on a vertical plane at $x = 0$ for different cavity sizes.

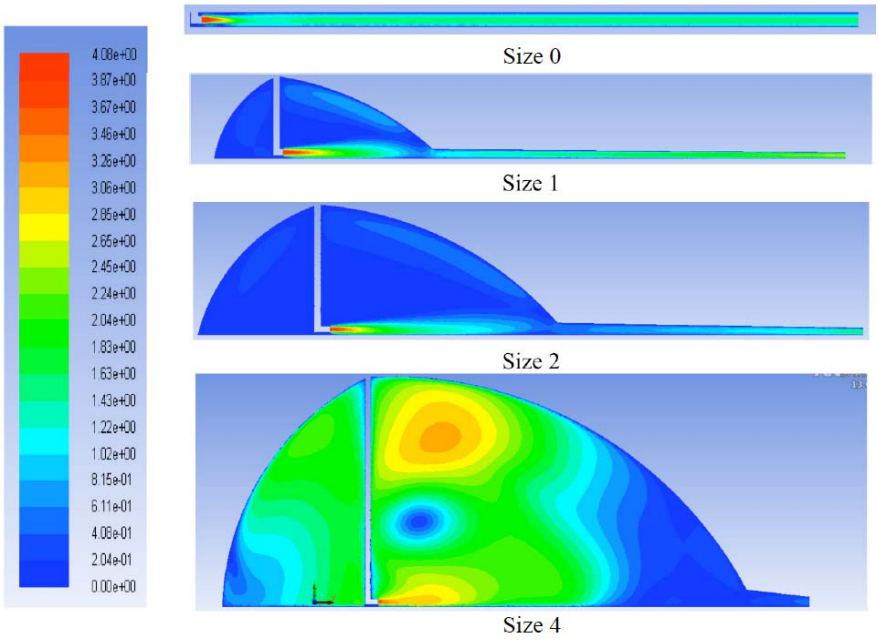

Figure 7: Velocity magnitude contours (in m/s) for horizontal injection on a center plane at z = 0 for different cavity sizes.

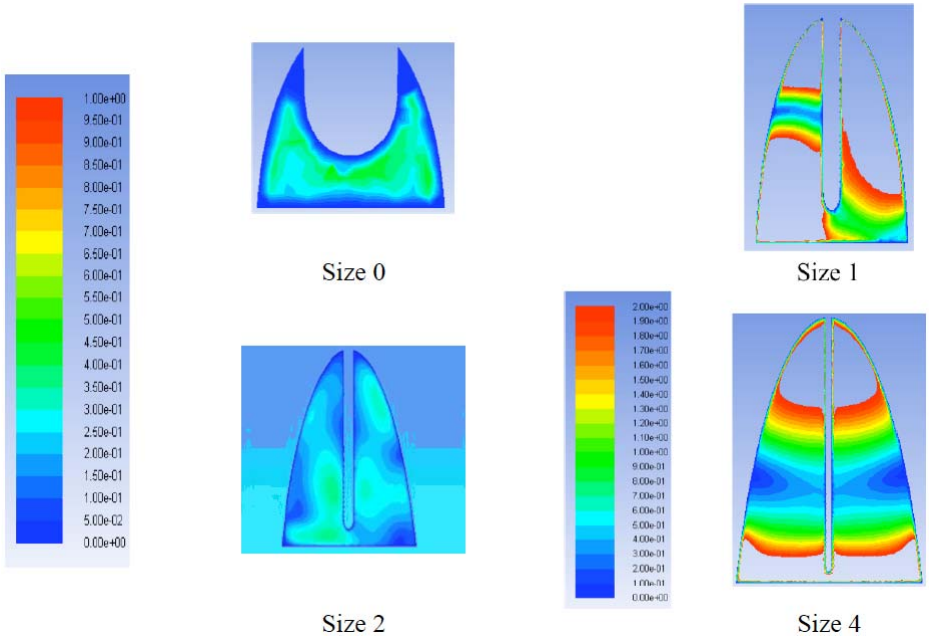

Figure 8: Velocity magnitude contours (in m/s) for inclined injection on a vertical plane at *x* = 0 for different cavity sizes.

CONCLUSIONS

The steady flow patterns inside the UCG cavity are studied numerically using a finite volume based solver. The hydrodynamics associated with the UCG process is understood with the help of a simplified fluid flow model. Following are some itemized observations from the present study:

- As the cavity size increases i.e. as the UCG process proceeds, the overall average value of the velocity magnitude decreases irrespective of the type of injection;
- A well mixed flow distribution is observed in the case of inclined injection;
- For vertical injection, the maximum velocity zones occur only at the inlet, whereas, for the case of horizontal injection it also occurs near the roof of the cavity due to recycling of the stream from the entrance of the outflow channel;

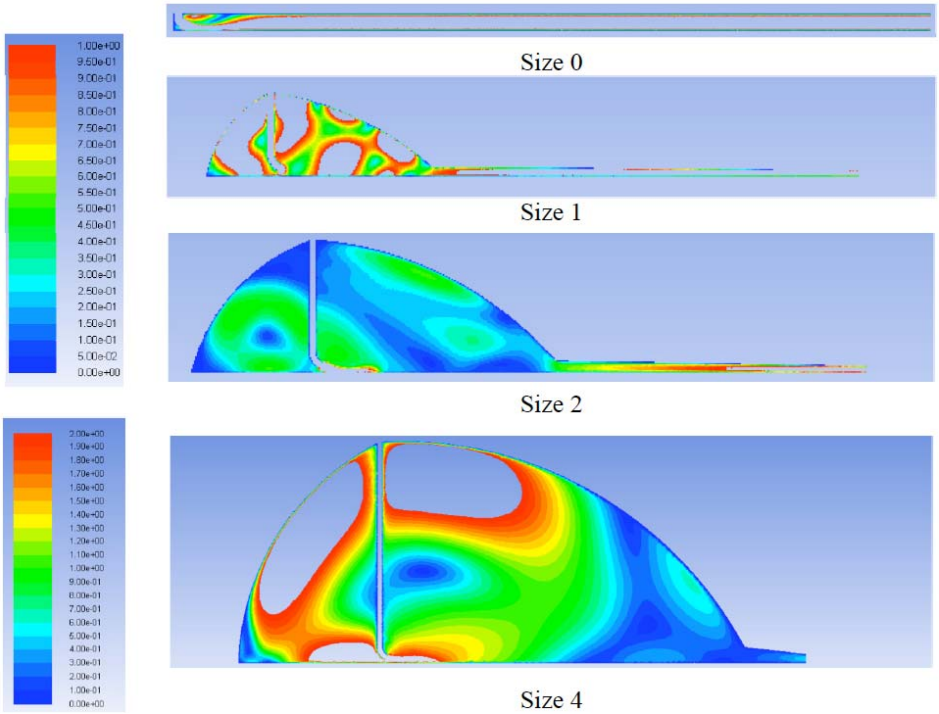

Figure 9: Velocity magnitude contours (in m/s) for inclined injection on a center plane at z = 0 for different cavity sizes.

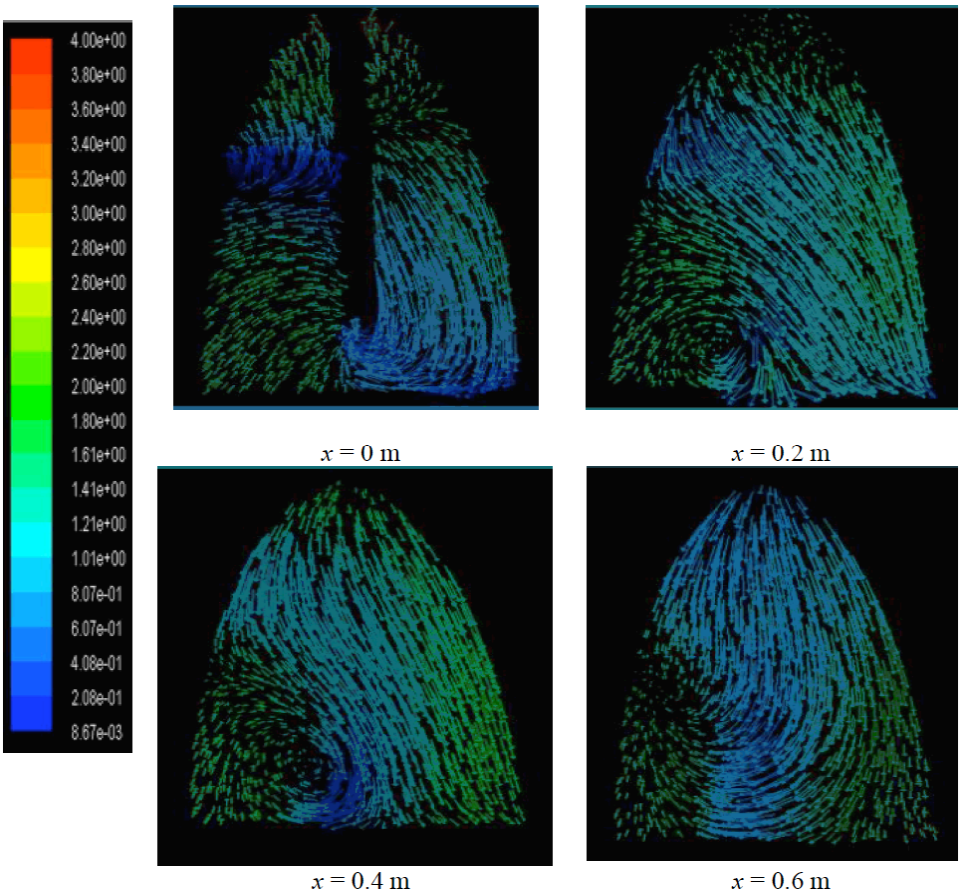

Figure 10: Velocity vectors (in m/s) for inclined injection for cavity size 1 at different vertical planes.

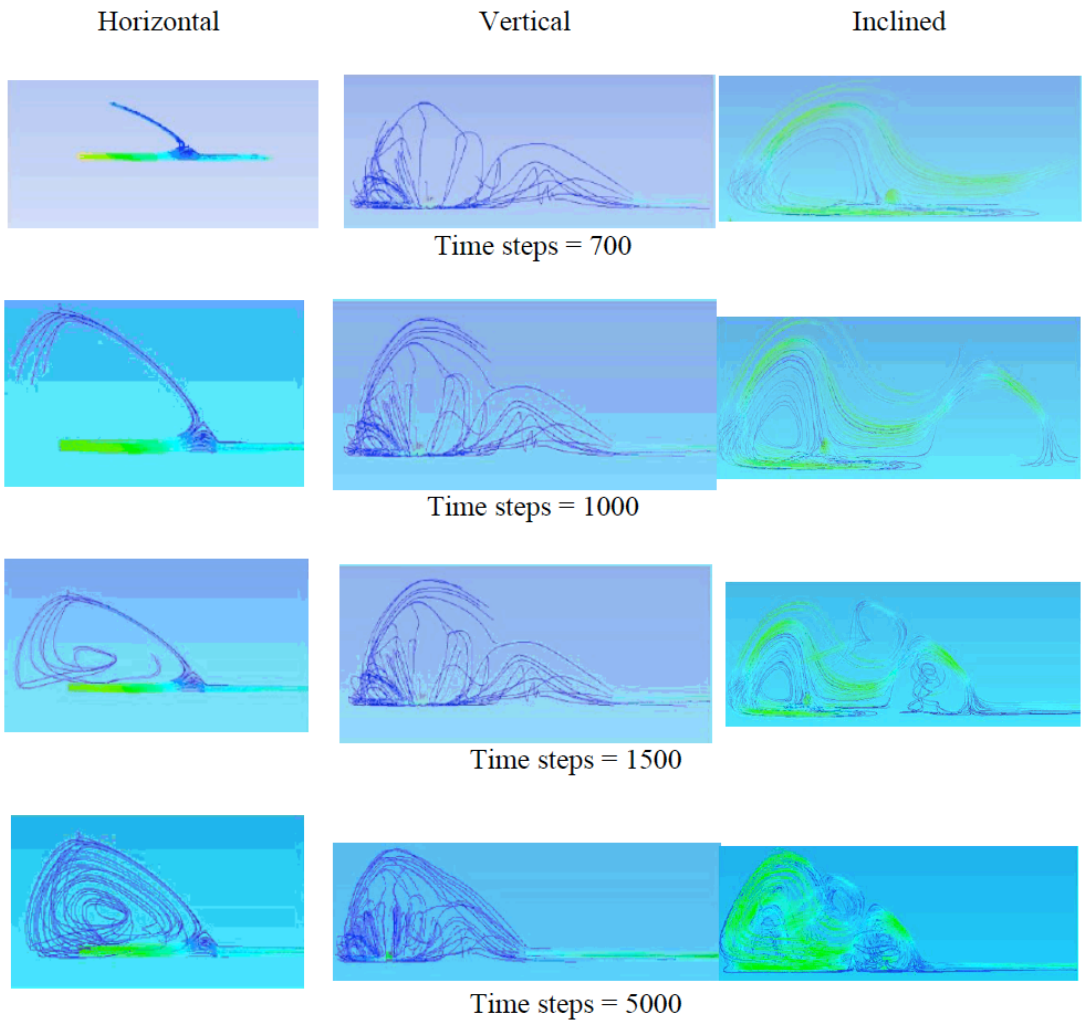

Figure 11: Pathlines colored by velocity magnitude (in m/s) at different time steps and different nozzle orientations for cavity size = 1 at *z* = 0 plane.

- Apart from the maximum velocity zones near the inlet and the roof of the cavity, for the case of inclined injection, they also occur on the left side of the cavity. It is because the nozzle imparts velocity in both *x*- and *y*-directions;
- Back mixing is more evident near the inlet but as one moves away towards the outflow channel, it decreases;
- For horizontal injection, a relatively larger portion of the pathlines behave like a parallel side stream and separately leave the cavity through the outflow channel. However, for the case of vertical injection the pathlines first hit the base of the cavity and the reflected pathlines leave the cavity through the outflow channel. Inclined injection shows both the properties and a better mixing is observed. Hence, the inclined injection is found to be the most preferable.

ACKNOWLEDGEMENT

The work was supported by CSIR, Govt. of India through the XII-th five year plan project "CoalGasUrja" under Engineering Cluster (project no. ESC0302).

REFERENCES

[1] Imran M, Kumar M, Kumar N, Qayyum A, Saeed A, Bhatti M. S. Environmental concerns of underground coal gasification. Renewable and Sustainable Energy Reviews 2011; 31: 600-610. http://dx.doi.org/10.1016/j.rser.2013.12.024

[2] Aghalayam P. Underground coal gasification: A clean Coal Technology, Handbook of combustion. Wiley-VCH: New York 2010; Vol. 5: pp. 257-275.

[3] Hadi AA, Hafez EA. Computer modeling of under-ground coal gasification. Science and Engineering 1986; 46(11).

[4] Wachowicz J, Janoszek T, Iwaszenko S. Model Tests of the Coal Gasification Process. Archives of Mining Sciences 2010; 55: 249-262.

[5] Perkins G, Sahajwalla V. A numerical study of the effects of operating conditions and coal properties on cavity growth in

Underground Coal Gasification. Energy and Fuels 2006; 20: 596-608. http://dx.doi.org/10.1021/ef050242q

[6] Yang L. Numerical simulation on three-dimensional nonlinear and unstable seepage of fluid in underground coal gasification, Fuel Processing Technology 2003; 84: 79-93. http://dx.doi.org/10.1016/S0378-3820(03)00047-X

[7] Yang L. Study on the model experiment and numerical simulation for underground coal gasification. Fuel 2004; 83: 573-584. http://dx.doi.org/10.1016/j.fuel.2003.08.011

[8] Yang L. Numerical study on the underground coal gasification for inclined seams. Environmental and Energy Engineering 2005; 51: 3059-3071.

[9] Yang L, Liu S. Numerical simulation on heat and mass transfer in the process of underground coal gasification. Numerical Heat Transfer, Part A 2003; 44: 537-557. http://dx.doi.org/10.1080/713838251

[10] Prabu V, Jayanti S. Simulation of cavity formation in underground coal gasification using bore hole combustion experiments. Energy 2011; 36: 5854-5864. http://dx.doi.org/10.1016/j.energy.2011.08.037

[11] Daggupati S, Mandapati RP, Mahajani SM, Ganesh A, Sapruc RK, Sharma RK, Aghalayama P. Laboratory studies on cavity growth and product gas composition in the context of underground coal gasification. Energy 2011; 36: 1776-1784. http://dx.doi.org/10.1016/j.energy.2010.12.051

[12] Prabua V, Jayanti S. Heat-affected zone analysis of high ash coals during *ex situ* experimental simulation of underground coal gasification. Fuel 2014; 123: 167-174. http://dx.doi.org/10.1016/j.fuel.2014.01.035

[13] Park KY, Edgar TF. Modeling of early cavity growth for underground coal gasification. Industrial and Engineering Chemistry Research 1987; 26: 237-246. http://dx.doi.org/10.1021/ie00062a011

[14] Harloff GJ. Underground coal gasification cavity growth model. Journal of Energy 1983; 7: 410-415. http://dx.doi.org/10.2514/3.62671

[15] Britten JA, Thorsness CB. A model for cavity growth and resource recovery during underground coal gasification. In Situ 1989; 13: 1-53.

[16] Perkins G, Sahajwalla V. A mathematical model for the chemical reaction of a semi-infinite block of coal in underground coal gasification. Energy and Fuels 2005; 19: 1679-1692. http://dx.doi.org/10.1021/ef0496808

[17] Perkins G, Sahajwalla V. Steady-state model for estimating gas production from underground coal gasification. Energy and Fuels 2008; 22: 3902-3914. http://dx.doi.org/10.1021/ef8001444

[18] Daggupati S, Mandapati RN, Mahajani SM, Ganesh A, Pal AK, Sharma RK, Aghalayam P. Compartment modeling for flow characterization of underground coal gasification cavity. Industrial and Engineering Chemistry Research 2011; 50: 277-290. http://dx.doi.org/10.1021/ie101307k

[19] Yang D, Sarhosis V, Sheng Y. Thermal–mechanical modelling around the cavities of underground coal gasification. Journal of the Energy Institute 2014; (In press). http://dx.doi.org/10.1016/j.joei.2014.03.029

[20] FLUENT 6.0 User's Guide, Fluent Inc., Lebanon, NH 2001.

[21] Incropera FP, DeWitt DP. Fundamentals of heat transfer, 5th Ed., Wiley 2001.

Received on 24-07-2014 Accepted on 22-08-2014 Published on 17-10-2014

DOI: http://dx.doi.org/10.15377/2409-5826.2014.01.01.3